Adipocyte

ISSN: (Print) (Online) Journal homepage: www.tandfonline.com/journals/kadi20

Effects of alpelisib treatment on murine *Pten*-deficient lipomas

Lea M. Merz, Karsten Winter, Sandy Richter, Sonja Kallendrusch, Andreas Horn, Sonja Grunewald, Nora Klöting, Kerstin Krause, Wieland Kiess, Diana Le Duc & Antje Garten

To cite this article: Lea M. Merz, Karsten Winter, Sandy Richter, Sonja Kallendrusch, Andreas Horn, Sonja Grunewald, Nora Klöting, Kerstin Krause, Wieland Kiess, Diana Le Duc & Antje Garten (2025) Effects of alpelisib treatment on murine *Pten*-deficient lipomas, Adipocyte, 14:1, 2468275, DOI: 10.1080/21623945.2025.2468275

To link to this article: https://doi.org/10.1080/21623945.2025.2468275

ADIPOCYTE
2025, VOL. 14, NO. 1, 2468275
https://doi.org/10.1080/21623945.2025.2468275

Taylor & Francis
Taylor & Francis Group

RESEARCH ARTICLE

OPEN ACCESS Check for updates

Effects of alpelisib treatment on murine *Pten*-deficient lipomas

Lea M. Merz[a], Karsten Winter[b], Sandy Richter[a], Sonja Kallendrusch[b,c], Andreas Horn[b], Sonja Grunewald[d], Nora Klöting[e], Kerstin Krause[f], Wieland Kiess[a], Diana Le Duc[g], and Antje Garten[a]

[a]Center for Pediatric Research, University Hospital for Children & Adolescents, Leipzig University, Leipzig, Germany; [b]Institute of Anatomy, Leipzig University, Leipzig, Germany; [c]Institute of Clinical Research and Systems Medicine, Health and Medical University Potsdam, Potsdam, Germany; [d]Department for Dermatology, Venereology and Allergology, University Hospital Leipzig, Leipzig, Germany; [e]Helmholtz Institute for Metabolic, Obesity and Vascular Research (HI-MAG), Helmholtz Center Munich at the University and University Hospital Leipzig, Leipzig, Germany; [f]Department of Endocrinology, Nephrology and Rheumatology, University Hospital Leipzig, Leipzig, Germany; [g]Institute of Human Genetics, University Hospital Leipzig, Leipzig, Germany

ABSTRACT

Phosphatase and tensin homolog (PTEN) hamartoma tumour syndrome (PHTS) is a rare disorder caused by germline mutations in the tumour suppressor gene PTEN, a key negative regulator of phosphatidylinositol 3-kinase (PI3K)/AKT signalling. Children with PHTS often develop lipomas, for which only surgical resection is available as treatment. We investigated the effects of the selective PI3K-inhibitor alpelisib on Pten-deficient lipomas. After incubation with alpelisib or the non-selective PI3K inhibitor wortmannin, we analysed histology, gene expression, and Pi3k pathway in lipoma and control epididymal adipose tissue (epiWAT). Alpelisib increased adipocyte area in lipomas compared to epiWAT. Baseline gene expression showed higher levels of markers for proliferation (*Pcna*), fibrosis (*Tgfb1*), and adipogenesis (*Pparg*) in lipomas, while hormone-sensitive lipase expression was lower than in epiWAT. Following alpelisib incubation, target genes of Pi3k signalling and extracellular matrix factors were reduced. We confirmed Pi3k inhibition through detecting decreased Akt levels compared to control treatment. Human lipoma samples treated with alpelisib showed variable lipolysis responses, suggesting variability in therapeutic outcomes. We established an ex vivo model to study alpelisib effects on Pten-deficient lipomas. These results underscore the therapeutic potential of targeted PI3K inhibition in the treatment of PHTS-associated lipomas, particularly in cases that are inoperable.

ARTICLE HISTORY
Received 25 September 2024
Revised 20 January 2025
Accepted 31 January 2025

KEYWORDS
Adipose tissue; phosphatidylinositol 3-kinase; phosphatase and tensin homolog; tissue slice culture; wortmannin

Introduction

Phosphatase and tensin homolog (PTEN) hamartoma tumour syndrome (PHTS) is a group of rare heterogeneous disorders caused by germline mutations in the tumour suppressor gene, *PTEN*. The corresponding protein is a dual lipid and protein phosphatase that dephosphorylates phosphoinositide substrates to decrease intracellular levels of phosphatidylinositol-3,4,5-trisphosphate (PIP3), thereby counteracting phosphatidylinositol 3-kinase (PI3K) (Figure 1a). Through phosphoinositide-dependent kinase 1 (PDPK1), PIP3 activates AKT, which subsequently increases mTOR signalling. PTEN is a major negative regulator of the PI3K/AKT/mTOR signalling pathway, which plays a crucial role in cell growth and cellular energy metabolism [1–3](Figure 1a). By inhibiting PI3K/AKT signalling, PTEN has been demonstrated to suppress tumour formation [4]. The PI3K/AKT pathway plays a critical role in regulating adipose tissue growth and remodelling, as evidenced by the fact that patients with PHTS not only face a high risk of malignancies but also commonly develop lipomas [5,6]. Subcutaneous or visceral lipomas are frequent and are observed in up to 39% of patients [7,8]. Lipoma growth can impede organ function, leading to acute or chronic life-threatening symptoms such as respiratory dysfunction or malnutrition [9,10]. Surgical excision remains the only treatment option for lipomas in PHTS patients. However, in some cases, the position of these lipomas renders them inoperable and resected lipomas have a high risk of recurrence. In addition to pathogenic *PTEN* variants in patients with PHTS, multiple sporadic malignancies also exhibit *PTEN* alterations [11]. Therefore, it is crucial to establish systemic therapeutic strategies to mitigate the effects of impaired *PTEN* activity.

Alpelisib (BYL719) is a selective inhibitor of the p110α catalytic subunit of PI3K and a potential drug

CONTACT Antje Garten antje.garten@medizin.uni-leipzig.de Center for Pediatric Research, University Hospital for Children & Adolescents, Central Research Building, Haus C, Liebeigstrasse 19, Leipzig 04013, Germany
Supplemental data for this article can be accessed online at https://doi.org/10.1080/21623945.2025.2468275

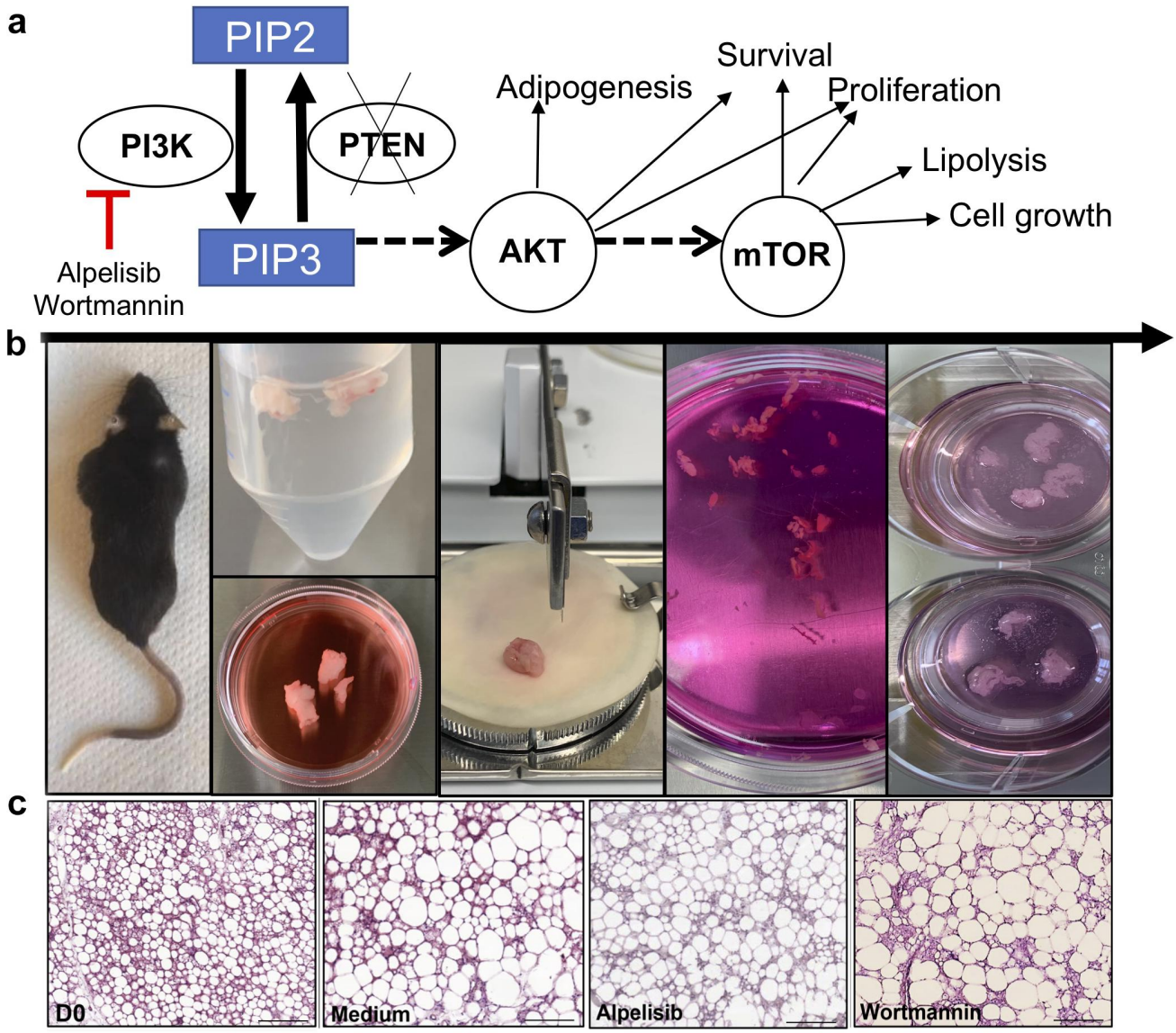

Figure 1. Schematic overview of PI3K/AKT/mTOR pathway and experimental design. a) PI3K activation induces conversion of phosphatidylinositol-4,5-bisphosphate (PIP2) to phosphatidylinositol-3,4,5-trisphosphate (PIP3). PIP3 is bound by AKT leading to AKT activation. Activated AKT indirectly stimulates mTOR regulating proliferation, lipolysis, adipogenesis, cell survival and growth. Alpelisib and wortmannin are direct inhibitors of PI3K. PTEN counteracts PI3K by dephosphorylating PIP3 to PIP2. b) Representative image of a 12- week-old homozygous Osx-Cre; *Rb1*$^{fl/fl}$; *Pten*$^{fl/fl}$ mouse with an axillary lipoma. Second column: 2 lipomas in PBS (upper image) and matching epiWAT control tissue in culture media (lower image). Third column: lipoma on sterile filter membranes before cutting with tissue chopper. Fourth column: 500 µm thick lipoma slices in culture media. Fifth column: 3 lipoma slices cultured on liquid-air-interface. c) Representative H&E staining of lipoma tissue cross sections from d0 and treatment conditions (control, alpelisib and wortmannin) after 72 h of incubation. Scale bar = 100 um. Tissue heterogeneity and morphology is well maintained across all conditions.

for the treatment of *Pten* deficient lipomas and other associated malignancies [12]. The first clinical study showed that the administration of alpelisib could successfully reduce the size of malignant and benign tumours [13,14]. For example, alpelisib has been approved for patients with *PIK3CA* mutated, advanced, or metastatic breast cancer [13]. Moreover, alpelisib treatment improved the clinical condition of patients with CLOVES syndrome, a rare genetic disorder caused by gain-of-function mutations in *PIK3CA* gene [15–19]. The symptoms include congenital lipomatous overgrowth, complex vascular malformations, epidermal naevi, skeletal abnormalities, and scoliosis. Patients treated with alpelisib demonstrated a volume reduction in vascular tumours, a decrease in hemihypertrophy, and improvements in scoliosis symptoms

[14]. Several studies have confirmed the beneficial effects of alpelisib in patients with *PIK3CA*-related overgrowth syndrome [15–19]. Moreover, alpelisib treatment induces tumour alterations in nude mice with *PIK3CA*-driven tumours, ranging from tumour stasis to regression [12]. In contrast to alpelisib, wortmannin is a steroid fungal metabolite that acts as a pan-selective irreversible PI3K inhibitor. Patients suffering from incurable solid tumours benefit from wortmannin-derived PX-866 as an add-on to conventional chemotherapy [20,21].

Based on the aforementioned studies, we hypothesized that alpelisib could be a promising new drug for the treatment of *Pten* deficient lipomas. We aimed to assess the pathobiology of *Pten* deficient lipoma and to compare the therapeutic efficacy of alpelisib with that of the pan-PI3K inhibitor wortmannin. In our previous work [9], we demonstrated that incubation of PTEN-haploinsufficient lipoma cells with alpelisib led to reduced proliferation and increased senescence. Building on these findings, we used *ex vivo* murine lipoma tissue slices in this study, which are a more physiological model compared to conventional 2D cell culture. This approach allowed us to assess the impact of alpelisib on adipocytes and progenitor cells within the tissue context. Using this model, we were able to determine adipocyte size, thereby gaining valuable insights into both adipocyte hypertrophy and hyperplasia. Additionally, by employing adipose tissue from the same mouse as an internal control, we were able to evaluate whether the observed effects of alpelisib were specific to lipoma tissue. This methodology provides a more comprehensive understanding of alpelisib's effects on lipoma tissue and its potential therapeutic applications. Using mice with a conditional *Pten/retinoblastoma (Rb1)* knockout, we established an *ex vivo* lipoma slice culture model and compared it with the epigonadal white adipose tissue (epiWAT) from the same mouse [22]. We used a semi-automated technique to assess adipocyte size, which revealed an increase in lipoma adipocyte area following alpelisib treatment. Gene expression analysis showed higher expression of the proliferation marker *proliferating cell nuclear antigen (Pcna)*, *transforming growth factor beta* (*Tgfb1)* and adipogenic transcription factor *peroxisome proliferator-activated receptor* (*Pparg)* in lipoma than in epiWAT control tissue. *Lipe* encoding hormone sensitive lipase was expressed at significantly lower levels in lipoma and reduced further by alpelisib incubation. Compared to wortmannin, alpelisib had a greater impact on AKT and on genes involved in lipolysis regulation. In conclusion, we established an *ex vivo* model of *Pten*-deficient lipomas and explored the therapeutic potential of targeted PI3K inhibition. Given the recurrence risk and limited systemic options, addressing PI3K/AKT signalling dysregulation through selective inhibitors like alpelisib offers a novel avenue for therapeutic intervention.

Methods

This study adhered to ARRIVE guidelines, please see checklist (Supplementary Table S1).

Mouse breeding and tissue collection

Osx-Cre:$Rb1^{fl/fl}Pten^{fl/fl}$ mice were bred by crossing $Pten^{fl/fl}$ (Stock B6.129S4-Ptentm1Hwu/J 006440, Jackson Labs) with *Osx*-Cre:$Rb1^{fl/fl}$ mice that were transgenic for a Tet-off GFP:Cre fusion construct under transcriptional regulation of the *Osterix(Osx)/Sp7* promoter (B6.Cg-Tg(Sp7-tTA,tetO-EGFP/cre)1Amc/J, kindly provided by Dr. Stuart H. Orkin, Boston Children's Hospital) [23,24]. Mice were housed and handled, and animal studies were conducted according to guidelines approved by the local authorities of the State of Saxony, Germany, and by the local animal ethics review board (Landesdirektion Leipzig, Germany; approval number TVV30/19).

The mice were housed under pathogen-free conditions, with 12 h of light per day and unlimited access to rodent chow and water. During breeding, *Cre* expression was suppressed using chow containing 625 mg/kg doxycycline (A112D70624; Ssniff Spezialdiäten, Soest, Germany). Male and female non-randomized mice were used for the experiments. At 3 weeks of age, *Cre* induction was achieved by weaning the mice into normal chow. Genotyping of *Pten* and *Rb* loxp sites and *Cre* transgene expression was carried out as previously described [22,25,26]. Within 4 weeks of switching to normal chow, Cre-positive mice started to develop uni- or bilateral non-invasive lipomas in the axillary region [24,26,27] (Figure 1b, first column). Mice were sacrificed by cervical dislocation and dissected between 15 and 24 weeks of age. We determined baseline gene expression differences between untreated lipoma and control WAT tissues from eight mice. For histological and gene expression analysis after 72 h of inhibitor treatment, lipomas and control epiWAT from six mice (four males and two females) were used. To evaluate pathway activation via western blot analysis, after 72 h of inhibitor treatment, lipomas and control epiWAT were obtained from five mice (one male, four females).

Tissue slice culture preparation and treatment

After reaching an average size of 5 × 10 mm, the lipomas and epiWAT were excised and placed on sterile filter membranes. As previously described [28], tissue was cut into 500 µm thick slices using a tissue chopper (McIlwain TC752, Campden Instruments, Loughborough, UK, or Saur, Reutlingen, Germany, Figure 1b, second and third column). Lipoma tissues and control epiWAT from each mouse were directly frozen in liquid nitrogen or fixed in 4% PFA for day 0. Subsequently, three slices were carefully transferred to an insert on a liquid-air-interface in a 6-well plate (Corning, New York, USA) and cultured at 37°C with a CO_2 content of 5% (Figure 1b, fourth to fifth column). Lipoma tissue and epiWAT were cultured in serum-free media containing Dulbecco's Modified Eagle's medium (DMEM), insulin-transferrin-selenium mixture (ITS), and penicillin/streptomycin (PenStrep) [28]. The culture medium was then replaced for 48 h. Slices were incubated with alpelisib (50 µM), wortmannin (100 µM) (Selleck Chemicals GmbH, Cologne, Germany), culture medium, or DMSO (0.1%) for 24 h. After inhibitor incubation for 72 h, the slices were fixed in 4% PFA for histological analysis or snap-frozen for RNA or protein isolation. The selected concentrations and timeframe were based on previous studies conducted by our group and others, as well as optimization experiments designed to enhance detection of inhibitor effects while preserving tissue viability.

Imaging

After fixation for over 24 h in 4% PFA, the slices were embedded in paraffin. Sections (10 µm) were cut, dewaxed, dehydrated in an alcohol series, and stained with haematoxylin and eosin. Whole 10 µm-thick slices were visualized using a digital slide scanner (Pannoramic Scan II, 3D HISTECH Ltd., Budapest, Hungary). To assess tissue integrity, haematoxylin and eosin (H&E) staining was performed, and 20 images per condition were manually inspected. Adipocytes were detected and measured (mean adipocyte area and adipocyte diameter) using Mathematica (Version 13.2, Wolfram Research, Inc., Champaign, IL, USA) [29]. For each image colourized cell masks were overlayed to the original HE images and inspected to ensure correct automatic adipocyte detection. Distributions of adipocyte cell areas and mean diameters from different experiments were calculated and plotted as distribution curves. Cut-off values were determined at relevant curve intersections.

Reverse transcription quantitative PCR (RT-qPCR)

For RNA extraction, slices were snap-frozen in liquid nitrogen and extracted using an RNeasy Mini Kit (Qiagen GmbH, Hilden Germany). RNA (500 ng) was reverse-transcribed using M-MLV Reverse Transcriptase (Invitrogen, Thermo Fisher Scientific, Inc., Waltham, MA, USA). For quantitative RT-PCR, qPCR Master Mix Low ROX (TaqMan Mastermix FAST; Eurogentec, Liege, Belgium) or Absolute qPCR SYBR-Green Low ROX Mix (Thermo Fisher Scientific, Inc.) was used. Measurements were performed using an Applied Biosystems 7500 Real-Time PCR System (Thermo Fisher Scientific, Inc.) with the following settings: activation at 95°C for 15 min, 40 cycles of denaturation at 95°C for 15 s, annealing at 60°C for 30 s, and elongation at 72°C for 30 s. The relative copy number of each sample was calculated, in a first step normalized to the housekeeper gene *Tbp* (TATA box binding protein) and subsequently normalized to the DMSO control. The expression levels of multiple genes associated with lipolysis, adipogenesis, extracellular matrix remodelling, and PI3K target genes were quantified. Primer sequences used are listed in Supplementary Table S2.

Western blot

After snap-freezing, tissue slices were pooled, lysed using TissueLyser II (Qiagen), and electrophoretic separation by SDS polyacrylamide gel electrophoresis was performed. Using standard protocols, proteins were blotted onto nitrocellulose membranes, and immunoblotting was performed to measure the amount of phosphorylated and total protein. Information on the antibodies used can be found in Supplementary Table S3.

Human lipoma samples

Lipoma tissue samples were obtained after elective surgical removal of sporadic lipomas from eight healthy subjects (six males and two females, age range 34–72 years). Surgeries were performed in the Department of Dermatology, Venereology, and Allergology at the University Hospital Leipzig, Germany. This study adhered to the Declaration of Helsinki and all procedures were approved and monitored by the ethics committee of Leipzig University, Germany (380/16-ek). Written informed consent was obtained from all the subjects. H&E-stained tissue sections of each sample were examined by light microscopy to confirm that lipomas were of the conventional type, without any cellular or nuclear atypia.

Human adipocyte isolation and lipolysis assay

Adipocytes were isolated by collagenase digestion, as described previously [30,31]. Briefly, lipoma tissue (1–2 g) was washed twice with sterile PBS and cut into pieces of approximately 0.5 cm length. After digestion for 90 min in a 200 U/ml collagenase-HBSS solution (Sigma, #C5138) in a 37°C shaking water bath, the material was filtered through a nylon mesh (pore size 400 µm) and centrifuged at 1,100 rpm at room temperature for 5 min. To assay lipolysis [31], the floating adipocyte layer was transferred to a 1.5 ml Eppendorf tube. The infranatant was removed, and adipocytes were washed three times before adding 50 µL of packed adipocytes to 100 µL of preadipocyte isolation buffer (123 mm NaCl, 5 mm KCl, 1.3 mm CaCl2·2H20, 5 mm glucose (Sigma G7021), 100 mm HEPES (AppliChem A3268), 1% penicillin/streptomycin (PAA P11–010), 4% BSA, fraction V protease-free (SERVA 11,926)) containing 10 µM isoproterenol (Sigma, #I6504) or 0.1% DMSO as a solvent control [31]. After shaking for 2 h at 37°C, 50 µL of infranatant was removed and stored at −80°C until determination of released glycerol, according to manufacturer's instructions (Free Glycerol Kit (Sigma, #F6428), Glycerol Standard Solution (Sigma, #G7793). After removal of residual infranatant, adipocytes were stored at −80°C until protein isolation.

Statistical analyses

Sample size was not calculated a priori, but determined by mouse and human tissue availability. The persons conducting experiments and data analysis were aware of group allocation during the whole study. The cut-off value referring to the percentage of small and large adipocytes (Figure 2) was determined by calculating the curve intersection point of the probability density functions for the two groups.

Statistical analyses were performed using GraphPad Prism, version 10.1. Outliers were determined using ROUT analysis (GraphPad Prism) and testing for normal distribution was performed using Kolmogorov-Smirnov test and QQ plots. Significant differences between two groups of non-normally distributed data were tested with Mann-Whitney U test, for more than two groups we used Kruskal-Wallis analysis of variance (ANOVA) with Dunn's correction for multiple testing. Significant differences considering two independent factors (tissue type and treatments) were determined using two-way ANOVA with Dunnett's correction for multiple comparisons. For results normalized to the mean of the solvent control, which was set to 1, a one-sample *t*-test was used to test for significant differences from 1. Statistical significance was set at $p < 0.05$. For Western blot analysis, the bands were densitometrically analysed using Fiji/Image J [32]. Phosphorylated proteins were normalized to the corresponding total proteins, and α-tubulin was used to normalize the total proteins. Data are presented as mean ±SD, *n* numbers are provided in the figure legends.

Results

Murine lipoma adipocytes were smaller than control epiWAT adipocytes

We established an *ex vivo* lipoma slice culture model using lipomas and epiWAT from the same *Pten/Rb* conditional knockout mice. Morphological analysis revealed well-preserved tissue integrity under all the conditions (Figure 1c).

Previous studies have shown that human lipoma samples contain smaller adipocytes, most likely because of adipocyte hyperplasia [33]. First, we investigated whether this was the case in mouse lipoma and assessed the adipocyte area in untreated, uncultured lipoma, and epiWAT control tissue (day 0). Similar to the human lipoma samples, murine lipomas showed a higher number of small adipocytes (density median epiWAT 0.0003030, lipoma 0.00023, $p < 0.0001$). On day 0 before cultivation, lipoma adipocytes showed a density peak at an adipocyte area of 280 µm^2, whereas epiWAT adipocytes plateaued between 250 and 1300 µm^2 (Figure 2a). We determined 547.85 µm^2 as a cut-off value to compare adipocyte are distribution of the lipoma and epiWAT adipocytes. 29.9% of lipoma adipocytes exhibited an adipocyte area ≤547.85 µm^2, in comparison to control epiWAT adipocytes with 19.3% ≤547.85 µm^2 (Figure 2a). Next, we tested whether the adipocyte area distribution pattern changed after 72-hour incubation in medium or medium containing 0.1% DMSO and found that it did not. However, while control epiWAT adipocytes showed a similar size distribution after medium cultivation (density median epiWAT d0 0.0003030, after medium incubation 0.0003120, $p = 0.2034$; 1.66% less adipocytes with an area ≤547.85 µm^2), lipoma adipocytes showed a subtle area decrease (density median lipoma d0 0.00023, after medium incubation 0.000159, $p < 0.0001$; 4.8% more adipocytes with area ≤547.85 µm^2, 29.9% to 34.7%, Figure 2b).

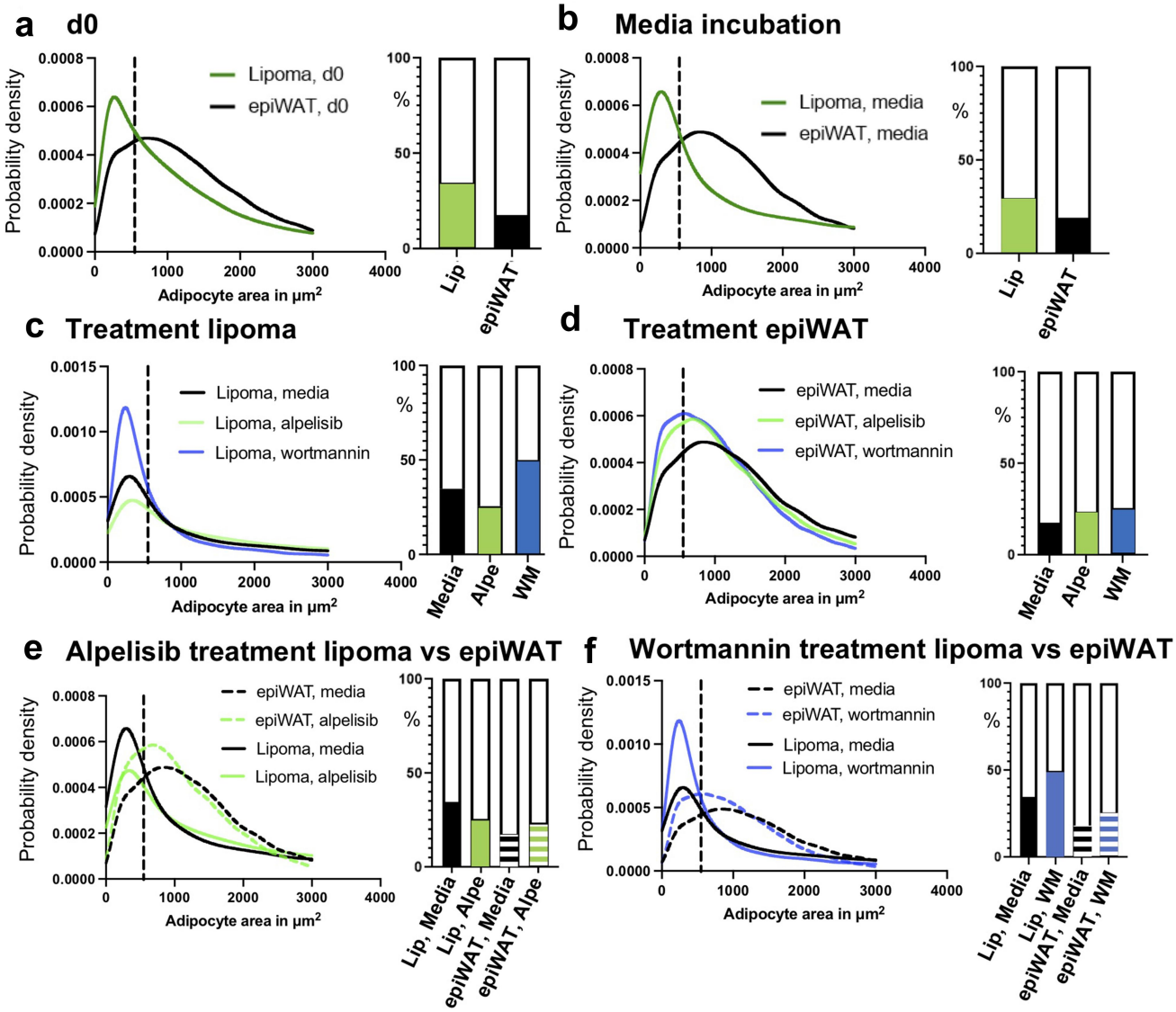

Figure 2. Adipocyte area in lipoma and epiWAT control tissue at d0 and after incubation with PI3K inhibitors. Each panel shows the area distribution curves on the left and the percentage of adipocytes below and above 547.85 µm^2 as bar charts on the right. The cut-off value of 547.85 µm^2 was determined by calculating the curve intersection point of the probability density functions for lipoma and epiWAT adipocytes and is indicated as a hatched line. The area distribution curves reflect the distribution of adipocyte area values within the sample, i.e. The probability of adipocyte area occurrence for any given adipocyte area value. In the accompanying bar charts, the percentage of adipocytes below/above 547.28 µm^2 is depicted. a) Lipoma tissue with higher number of small adipocytes compared to epiWAT at d0: before incubation lipoma adipocyte size peaked at 280 µm^2 compared to 250–1300 µm^2 in epiWAT. 29.9% of lipoma and 19.3% of epiWAT adipocytes exhibited a mean area ≤547.85 µm^2. b) epiWAT adipocytes after 72 h incubation in control medium showed similar size distribution as epiWAT adipocytes on d0, whereas lipoma adipocytes after 72 h incubation in control medium showed subtle area decrease (epiWAT: 1.66% less adipocytes ≤547.85 µm^2, lipoma: 4.7% less adipocytes ≤547.85 µm^2 after 72 h incubation in control medium). c) After 72 h incubation alpelisib-treated lipoma tissue showed subtle area increase (highest number of adipocytes in control medium: 280 µm^2, in wortmannin: 245 µm^2, in alpelisib 400 µm^2). Number of adipocytes ≤547.85 µm^2 decreased by 9.1% in alpelisib-incubated slices compared to control medium incubation. Increase of lipoma adipocytes ≤547.85 µm^2 in wortmannin-incubated tissue compared to control medium incubation. d) After 72 h incubation, epiWAT slices both treated with alpelisib and with wortmannin showed a adipocyte area reduction (control medium: 400–1600 µm^2, alpelisib 400–1000 µm^2, wortmannin: 320–800 µm^2). After alpelisib incubation, epiWAT adipocytes ≤547.85 µm^2 increased by 5.8% compared to control medium (control medium 17.7%, alpelisib 23.5%). After wortmannin incubation, epiWAT adipocytes ≤547.85 µm^2 increased by 8.2% (control medium 17.7%, wortmannin 25.9%). e) Comparison of changes of adipocyte area of epiWAT and lipoma tissue slices after 72 h E) alpelisib incubation and f) wortmannin incubation.

The number of larger lipoma adipocytes increased after alpelisib incubation

Next, we hypothesized that alpelisib treatment would cause a change in adipocyte size. We expected either a size increase, as inhibition of Pik3 p110α could potentially suppress progenitor cell proliferation, or a decrease, caused by the induction of lipolysis via AKT inhibition [34]. We used the earlier determined cut-off point (547.85 μm^2) for comparing the adipocyte size distributions after incubation of tissue slices with alpelisib to control medium.

Interestingly, lipoma slices treated with alpelisib showed a subtle increase in mean adipocyte area (density median lipoma control 0.000159, density median lipoma after alpelisib incubation 0.000189, $p < 0.0001$) compared to solvent control treated lipoma slices. In control treated lipoma slices, the highest number of adipocytes had an area of 280 μm^2, the adipocyte area of alpelisib-treated lipomas peaked at approximately 400 μm^2 (Figure 2c,e). Furthermore, the number of adipocytes ≤547.85 μm^2 decreased by 9.1% (lipoma: control medium 34.7%, alpelisib 25.5%, Figure 2c,e). These findings suggest that alpelisib may simultaneously promote adipocyte hypertrophy and inhibit progenitor cell proliferation, pointing to a dual effect of alpelisib on lipomas. Control epiWAT slices treated with alpelisib showed the opposite results, with a decrease in the mean adipocyte area (density median epiWAT control 0.000312, density median epiWAT after alpelisib incubation 0.000301, $p = 0.0244$) compared to control treated slices. While epiWAT adipocytes incubated in control medium mostly had a size between 400 and 1600 μm^2, alpelisib incubation resulted in an increased number of epiWAT adipocytes between 400 and 1000 μm^2. Moreover, the number of adipocytes ≤547.85 μm^2 increased by 5.8% (epiWAT: control medium 17.7%, alpelisib 23.5%; Figure 2d,e).

In contrast to alpelisib, 72 h of wortmannin incubation led to a decrease in the mean adipocyte area in both lipomas (density median lipoma control 0.000159, density median lipoma after alpelisib incubation 0.000125, $p < 0.0001$) and epiWAT (density median epiWAT control 0.000312, density median epiWAT after alpelisib incubation 0.0003, $p = 0.0073$). Compared to control medium-incubated lipoma adipocytes with the highest number having an area of 280 μm^2, wortmannin-treated lipoma adipocytes peaked at an area of 245 μm^2. Moreover, the number of lipoma adipocytes with a mean area ≤547.85 μm^2 increased by 15.25% (34.7% in control medium-incubated vs. 49.9% in wortmannin-incubated, Figure 2c,f). The effect of wortmannin incubation was similar in epiWAT adipocytes, demonstrating an area reduction in wortmannin-treated slices (peak between 400 and 1600 μm^2) compared to control tissue (peak between 320 and 800 μm^2). The percentage of adipocytes ≤547.85 μm^2 increased from 17.7% to 25.9% (Figure 2d,f).

Notably, we additionally evaluated the density distributions of the diameter of lipoma and epiWAT adipocytes. Consistent distribution patterns were observed, showing similar effects of alpelisib and wortmannin incubation (Supplementary Figure S1a-f).

Baseline gene expression differs between lipoma and control WAT

Before examining the impact of alpelisib treatment on gene expression, we determined the basal gene expression differences between lipoma and epiWAT. We compared the expression of genes found to be differentially expressed in either human *PTEN* knockout adipose progenitor cells [35] or sporadic human lipoma [33] compared to the respective controls. Genes encoding proteins involved in adipogenesis regulation, lipolysis, and extracellular matrix remodelling were analysed (Figure 3a). We initially measured *Pten* expression levels, revealing an expected residual but significantly lower *Pten* expression in lipoma tissue (Figure 3a). Our data showed significantly higher expression levels of the proliferation marker *proliferating cell nuclear antigen (Pcna)* in lipoma (Figure 3a). Distinct patterns of gene expression were observed for adipogenic transcription factors: *peroxisome proliferator activated receptor gamma (Pparg)* expression was significantly elevated, while *sterol regulatory element binding transcription factor 1 (Srebf1)* expression was significantly decreased in lipoma compared to epiWAT. Similarly, we found a significant downregulation of *hormone sensitive lipase/lipase E (Lipe)*, but detected no difference in *adipose tissue triglyceride lipase/patatin-like phospholipase domain-containing protein 2 (Atgl/Pnpla2)* or *prostaglandin E receptor 3 (Ptger3)* expression (Figure 3a). *Lysyl oxidase (Lox)* and *elastin (Eln)* expression was significantly decreased, whereas the fibrosis marker *transforming growth factor beta (Tgfb1)* was increased in lipoma tissue, indicating extracellular matrix remodelling (Figure 3a).

Alpelisib effects gene expression in lipoma compared to epiWAT slices

Having identified three genes (*Pcna*, *Pparg*, *Tgfb1)* that show higher expression in lipoma than in control WAT, we aimed to investigate whether alpelisib

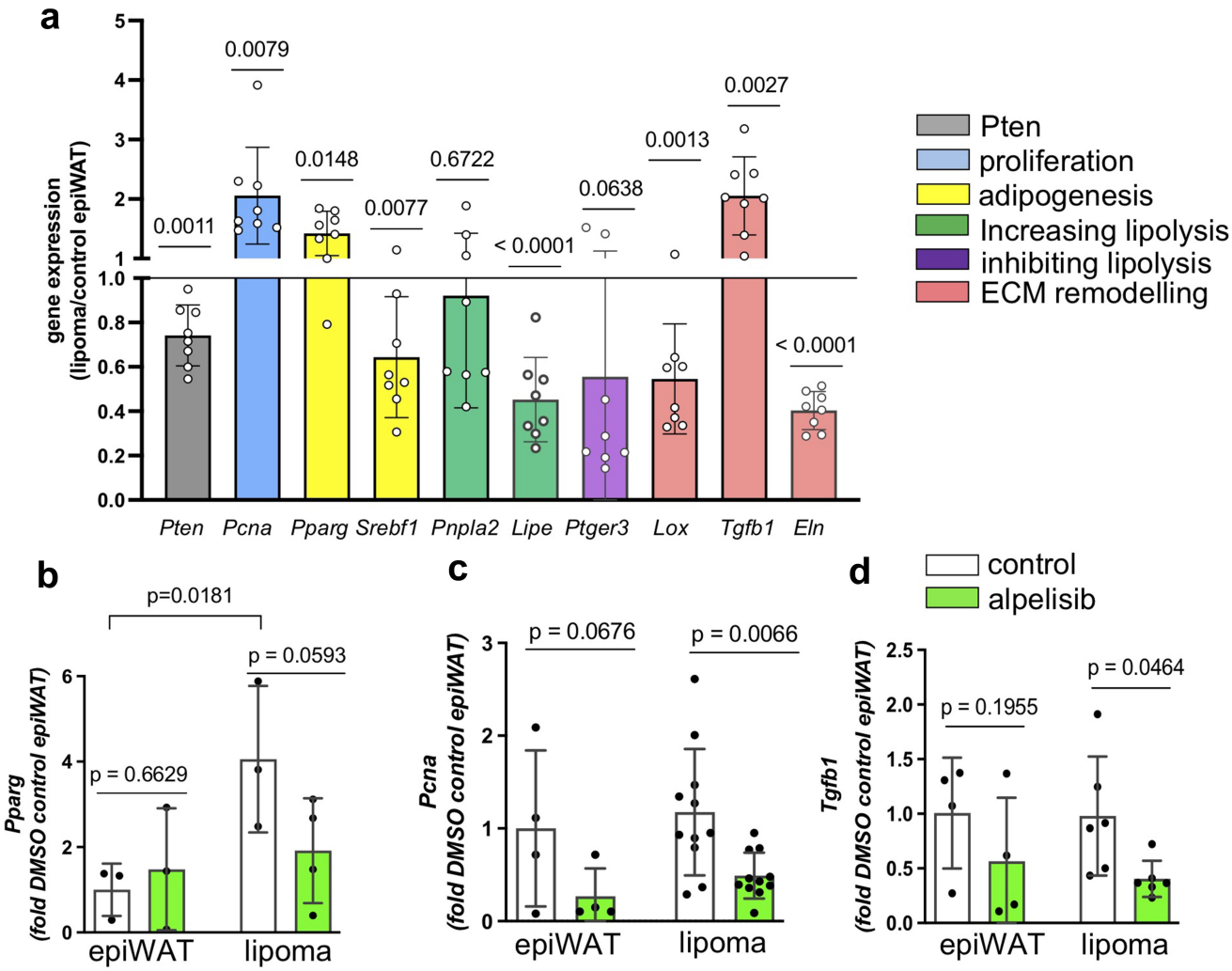

Figure 3. Gene expression patterns in *Pten* deficient lipoma versus epiWAT. a) Compared to control epiWAT, *Pten* was significantly lower expressed in lipoma tissue ($p = 0.001$), whereas *Pcna* ($p = 0.008$), *Pparg* ($p = 0.015$) and *Tgfb1* ($p = 0.003$) expression was elevated. *Srebf1* ($p = 0.008$), *Lipe* ($p < 0.0001$), *Lox* ($p = 0.0013$) and *Eln* ($p < 0.0001$) expression was significantly decreased in lipoma. No difference was detected in *Pnpla2* ($p = 0.672$) and *Ptger3* ($p = 0.0649$) expression levels, with a trend towards lower expression of *Ptger3*. Data are presented as fold changes lipoma/control adipose tissue, which is depicted by a line at 1 (mean±sd, $n = 7–8$ independent experiments). b-d) *Pparg*, *Pcna* and *Tgfb1* expression in alpelisib-treated versus control-treated lipoma and epiWAT slices. Expression of *Pcna* ($p = 0.0066$), *Tgfb1* ($p = 0.046$) and *Pparg* ($p = 0.059$) was significantly reduced in alpelisib-incubated compared to control incubated lipoma slices. Alpelisib-treated epiWAT slices did not show significant gene expression differences compared to control treatment, with a trend towards lower *Pcna* expression in alpelisib vs control-treated epiWAT. Data were normalized to the mean of solvent controls and presented as mean±sd ($n = 3–10$ independent experiments). Abbreviations: *Pcna* = proliferating cell nuclear antigen, *Tgfb1* = transforming growth factor beta, *Pparg* = peroxisome proliferator activated receptor gamma, *Srebf1* = sterol regulatory element-binding factor 1, *Lox* = lysyl oxidase, *Eln* = elastin, *Lipe* = hormone-sensitive lipase, *Pnpla2* = patatin-like phospholipase domain-containing protein 2.

treatment would affect gene expression differently in lipoma and control WAT. However, after 72 h of incubation with alpelisib, only *Pparg* showed a significant difference in expression between lipoma and control WAT (Figure 3b, $p = 0.0181$). Alpelisib incubation resulted in reduced *Pparg* expression compared to control medium in lipoma tissue (borderline significant, $p = 0.059$), while its effect on *Pparg* expression was less pronounced in control WAT. Our findings revealed a significant decrease in *Pcna* ($p = 0.0066$) and *Tgfb1* ($p = 0.0464$) expression in lipoma slices after incubation with alpelisib compared to control medium. In contrast, there was a trend towards reduced *Pcna* expression and no significant effect on *Tgfb1* expression in alpelisib-incubated compared to control-treated epiWAT (Figure 3c-d).

Next, we investigated gene expression changes in lipoma slices to compare the effects of the specific Pik3 p110α inhibitor alpelisib on pan-Pi3k inhibition

by wortmannin. We initially tested whether wortmannin incubation would be associated with effects on *Pcna* expression similar to those observed with alpelisib incubation. However, we observed no reduction in *Pcna* expression following wortmannin incubation (Figure 4a). Next, we tested two other Pi3k target genes, *Glut1 (glucose transporter 1)* and *Pgk1 (phosphoglycerate kinase 1)*. *Pgk1* expression was not significantly altered by either wortmannin or alpelisib treatment (Figure 4b). In contrast, *Glut1* expression was strongly upregulated after alpelisib treatment, whereas wortmannin treatment had no significant effect (Figure 4c, $p = 0.0005$) compared to control medium.

Next, we assessed whether alpelisib and wortmannin treatment would alter the expression of genes involved in extracellular matrix remodelling (*Tgfb1, Lox, Eln*). Slices treated with wortmannin did not show changes in expression of these genes. *Tgfb1* and *Eln* expression was reduced after alpelisib incubation (Figure 4d-e), whereas *Lox* expression was unchanged (Figure 4f) compared to control medium.

Our data indicated that alpelisib treatment was associated with increased mean adipocyte area in lipomas. The reduced number of smaller adipocytes after alpelisib incubation could be associated with downregulation of the proliferation marker *Pcna*. Another factor contributing to increased adipocyte size could be a decrease in lipolysis. Therefore, we examined the expression of the genes that regulate lipolysis. Expression of *patatin like phospholipase domain containing 2 (Pnpla2)* was unchanged (Figure 4g). Interestingly, the expression of both *Lipe* and *Ptger3*, which displayed lower expression in lipoma compared to epiWAT (Figure 3a), was further diminished in slices cultured with alpelisib compared to control medium (Figure 4h,i). *Guanine nucleotide-binding protein α subunit inhibitory (Gnai)* and *monoamine oxidase (Mao A* and *B*, Figure 4j-l) expression did not change significantly after alpelisib incubation. Similar to the lack of expression changes in Pi3k targets and ECM remodelling, we did not detect changes in the expression of lipolysis-related genes after wortmannin treatment (Figure 4j-l).

Akt and Hsl were reduced after alpelisib treatment in lipoma

Given the substantial differences in effects on gene expression between alpelisib and wortmannin treatment, we next evaluated the capacity of both inhibitors to reduce Akt phosphorylation, a downstream target of Pi3k. The amount of Pten protein was not affected by inhibitor treatment but, as expected, was lower in lipomas compared to control WAT (Figure 5a). Consistent with the reduced Pten levels, we observed increased Akt phosphorylation in lipoma tissues. Treatment with alpelisib, but not wortmannin, abrogated Akt phosphorylation in lipomas ($p = 0.0015$, Figure 5b). Moreover, total Akt was reduced after alpelisib treatment compared to control medium in both control and lipoma tissues ($p = 0.0447$ for control, $p = 0.07234$ for lipoma tissue, Figure 5c).

Hormone-sensitive lipase (Hsl) is one of the downstream targets of Akt and is activated when Akt phosphorylation is attenuated. Therefore, we investigated Hsl phosphorylation and found a significant increase in alpelisib-treated lipoma slices compared to control-treated lipoma slices ($p = 0.0001$, Figure 5d). Notably, we detected higher Hsl phosphorylation in lipoma compared to control WAT slices after alpelisib treatment ($p = 0.0105$, Figure 5d). We also observed a trend towards the downregulation of total Hsl protein following alpelisib treatment compared to control medium in lipomas ($p = 0.0578$, Figure 5e), supporting our findings from gene expression analysis (Figure 4h). In line with previous results, wortmannin treatment did not affect the activation of Hsl.

Alpelisib affected glycerol release from a subset of human lipoma adipocytes

Given our opposing observations of increased HSL phosphorylation but reduced total HSL protein in lipoma after alpelisib treatment, we wanted to examine the effect of alpelisib on glycerol release as an indicator of lipolysis. We used the supernatant obtained by changing the medium of the slice cultures after 48 h of incubation. We detected higher glycerol levels in epiWAT supernatants than in lipoma supernatants, with a difference in slices incubated with DMSO (borderline significant with $p = 0.0564$), but no significant differences between control and inhibitor treatments (Supplementary Figure S2A).

We examined glycerol release after alpelisib incubation in adipocytes isolated from human sporadic lipomas. The beta-adrenergic agonist isoproterenol served as a positive control for lipolysis. We found that unlike isoproterenol, alpelisib did not elicit a significant lipolytic response in human adipocytes ($p = 0.0002$ for isoproterenol, $p = 0.374$ for alpelisib, Figure 6a). Furthermore, alpelisib did not increase HSL phosphorylation ($p = 0.0006$ for isoproterenol and $p = 0.1583$ for alpelisib; Figure 6b).

For incubation with isoproterenol, the released glycerol showed a positive linear correlation with HSL phosphorylation, which was not observed for alpelisib

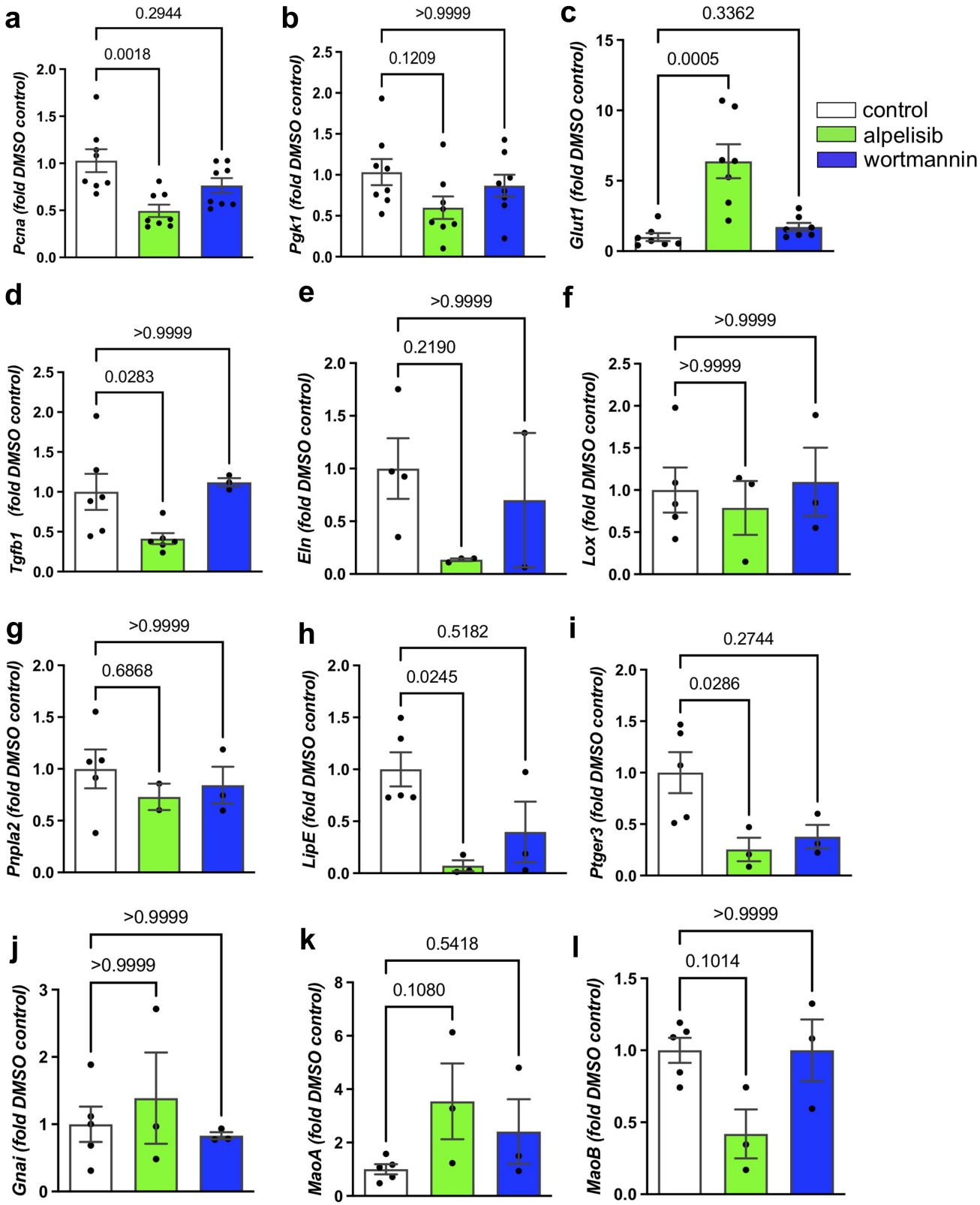

Figure 4. Expression differences of PI3K targets, genes involved in lipolysis and in extracellular matrix remodelling in alpelisib-treated lipoma. a) *Pcna* expression was reduced ($n = 8$), while b) *Pgk1* expression was not changed and c) *Glut1* expression was significantly elevated ($n = 7$) in lipoma tissue incubated with alpelisib compared to control-treated lipoma slices. Lipoma slices incubated with alpelisib exhibited d) reduced *Tgfb1* ($n = 6$) and e) *Eln* expression ($n = 3$), while F) *Lox* was not altered compared to control-treated lipoma tissue slices. G) *Pnpla2* and h) *Gnai* expression was not altered, in contrast i) *Lipe* ($n = 3$) and j) *Ptger3* ($n = 3$) expression was diminished after incubation with alpelisib compared to control treatment. Opposite effects were seen regarding k) *MAO A* and l) *MAO B* expression levels after alpelisib compared to control medium incubation. Lipoma slices incubated with wortmannin showed no gene expression changes compared to controls. Data were normalized to the mean of solvent controls and presented as mean±sem ($n = 2$–8 independent experiments).

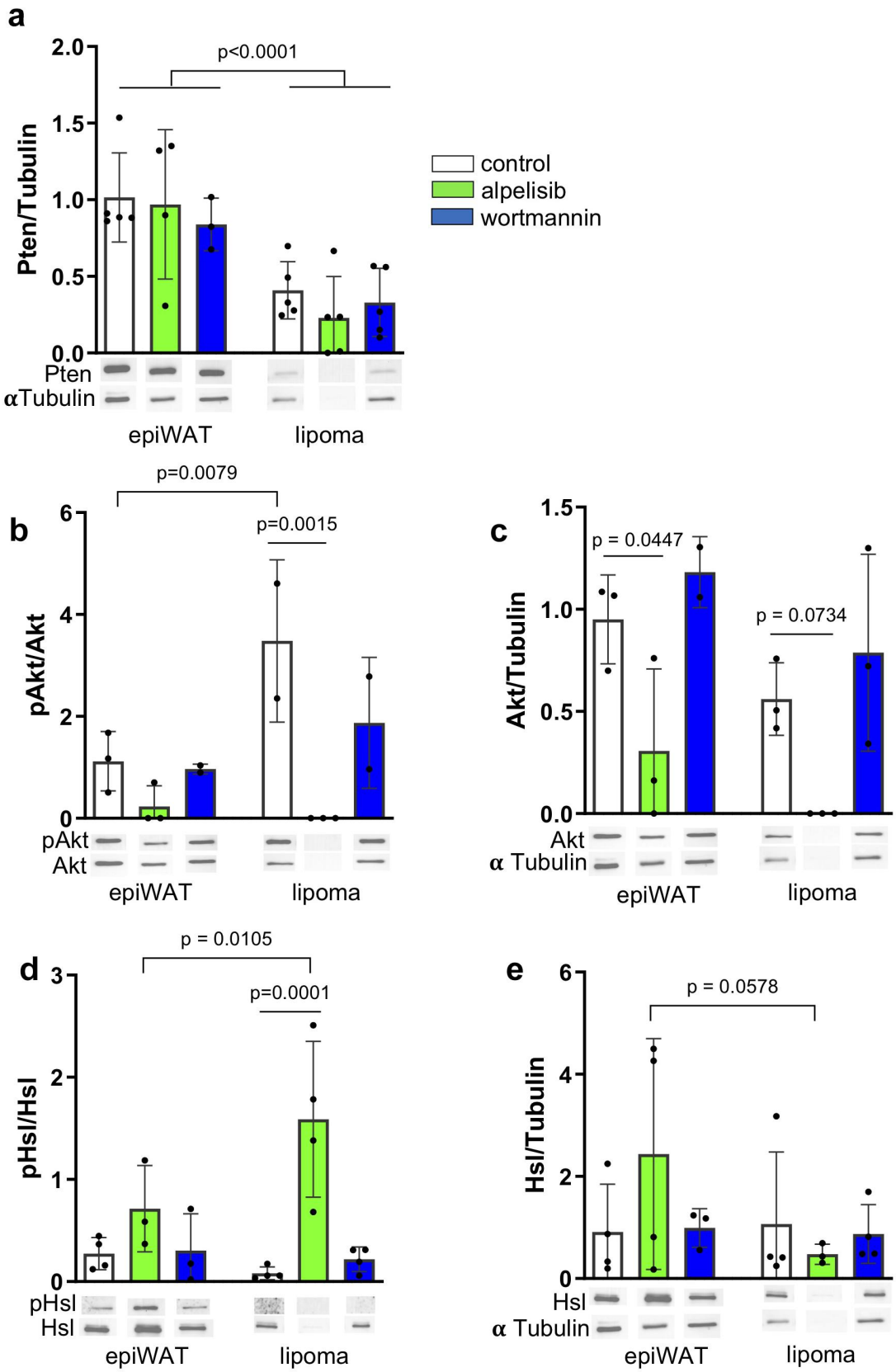

Figure 5. Pten, Akt and Hsl protein was altered by alpelisib treatment in lipoma and epiWAT. a) Pten protein was significantly reduced in lipoma tissue compared to epiWAT, regardless of inhibitor treatment. b) Phospho(Ser473)Akt was higher in lipoma compared to epiWAT slices after 72 h in control medium. Alpelisib incubation for 72 h reduced phospho(Ser473)Akt both in lipoma and epiWAT, with a significant difference in lipoma slices compared to control treatment ($n = 3$, $p = 0.0015$). c) Total Akt was

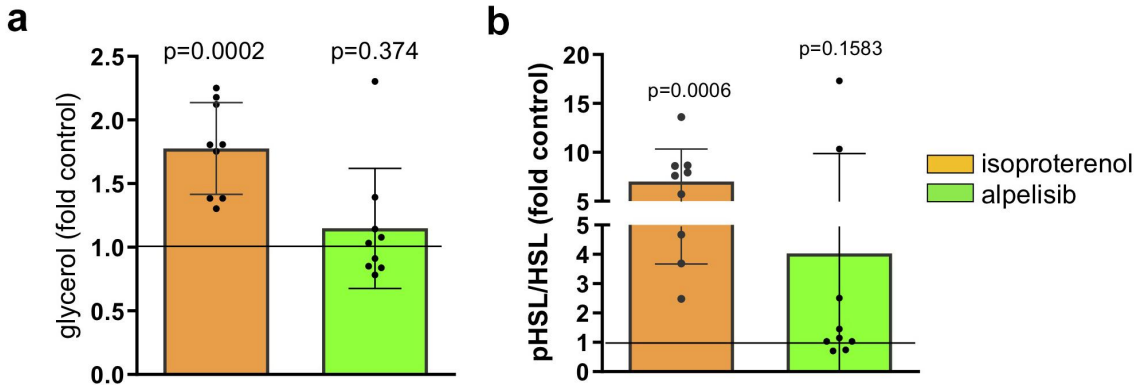

Figure 6. Lipolysis in human lipoma adipocytes is not influenced by alpelisib. a) Glycerol release and b) HSL phosphorylation in human lipoma adipocytes was significantly increased after isoproterenol incubation and remained unaltered following alpelisib incubation. Three out of nine human lipoma samples showed an increased glycerol release and corresponding HSL phosphorylation after treatment with alpelisib. Data were normalized to solvent control treated values for each experiment shown as line at 1 and presented as mean±sd of 9 independent experiments.

incubation ($r^2 = 0.362$ for isoproterenol, $r^2 = 0.003739$ for alpelisib; Supplementary Figure S2b, c).

Interestingly, individual experiments revealed that alpelisib incubation enhanced lipolysis in three out of the nine lipoma adipocyte samples. These three samples also showed an increase in phosphorylated HSL (lipomas #1, #3, and #8; Supplementary Table S4). Based on a limited sample size, we report that incubation with alpelisib induces lipolysis in a subgroup of human lipoma adipocytes.

Discussion

Patients with PHTS caused by germline *PTEN* variants are at an increased risk of adipose tissue overgrowth, which can severely diminish their quality of life. To date, no curative systemic treatment is available. We previously showed that alpelisib reduces the proliferation of *PTEN*-haploinsufficient lipoma cells *in vitro* [9]. Moreover, alpelisib has been shown to provide substantial benefits to patients with *PIK3CA*-related adipose tissue overgrowth [36]. To enhance our understanding of *PTEN*-deficient lipoma responses to alpelisib, we established an *ex vivo* murine *Pten*-deficient lipoma slice culture model. We assessed histological and baseline gene expression differences when comparing lipomas with control epiWAT. We then treated lipoma and epiWAT slices with the PI3K p110α-specific inhibitor alpelisib and the non-selective PI3K inhibitor wortmannin and subsequently analysed tissue histology, gene expression, protein abundance, and PI3K/AKT pathway activation.

In previous studies on human sporadic lipomas, we and others demonstrated an increase in smaller-sized adipocytes, which potentially occurs because of increased adipose progenitor cell proliferation [33,37]. Our current data show similar results, with an increased number of small adipocytes in untreated murine *Pten*-deficient lipoma tissue compared to that in epiWAT. In line with the hypothesis that adipose progenitor cell proliferation is increased in lipomas, we found that the proliferation marker *Pcna* is higher in lipomas than in control tissues. Alpelisib treatment caused a decrease in *Pcna* expression in lipomas and epiWAT, indicating attenuation of adipose progenitor cell proliferation in both tissues.

Kim *et al.* used a similar p110α-selective inhibitor (PIK-75) during *in vitro* adipocyte differentiation of 3T3-L1 cells and demonstrated downregulation of the adipogenic master transcription factor *Pparg* accompanied by attenuated adipocyte differentiation [38]. These findings align with our previous *in vitro* results on alpelisib exposure in human *PTEN* haploinsufficient lipoma cells, where we observed a reduction in lipoma cell growth and adipogenesis [9]. Similarly, in the

significantly reduced in both, lipoma and control tissue. d) Phospho(Ser660)Hsl levels were increased in alpelisib-treated lipoma and epiWAT tissue, with a significant increase in lipoma tissue compared to control-treated phospho(Ser660)Hsl and epiWAT. e) Total Hsl abundance tended to be reduced in lipoma compared to epiWAT. Wortmannin treatment did not induce significant differences in lipoma or epiWAT tissue compared to control treatment. Results from densitometric analyses of 2–4 independent experiments are shown as mean±sd with a representative Western blot image for each graph.

current study, *Pparg* was more highly expressed in lipoma than in control epiWAT and was significantly downregulated after alpelisib incubation. In epiWAT, alpelisib showed no effect on *Pparg* expression, suggesting a selective effect of p110α PI3K inhibition on lipoma adipocytes.

p110α is the main insulin-responsive catalytic PI3K subunit in the adipose tissue [39,40]. Mice overexpressing a constitutively active Pi3k p110α subunit develop adipose tissue overgrowth with increased adipocyte size and lipolysis reduction [36]. Moreover, Ladraa *et al.* found partial recovery of adipocyte size in alpelisib-treated mice [36]. Due to inhibition of proliferation or enhanced lipolysis in lipoma slices, we expected a reduction in the number of small adipocytes and adipocyte area following treatment. However, histological analysis revealed an increased adipocyte area in the lipoma slices following alpelisib treatment. In epiWAT slices, we observed a reduction in the adipocyte area after incubation with alpelisib. Interestingly, wortmannin administration caused a decrease in adipocyte size in both the lipoma and control tissues. The opposing effects of alpelisib and wortmannin on lipoma adipocyte size could be associated with their different selectivities. Alpelisib specifically binds to the PIK3 p110α subunit, whereas wortmannin is a pan-PI3K inhibitor that affects additional PI3K subunits (p110β, γ, and δ). Moreover, wortmannin inhibits enzymes involved in DNA repair, cell division, and mitosis, including DNA-dependent protein kinase (DNA-PK), ataxia telangiectasia (ATM), and polo-like kinase 1 (PLK1) [41,42]. Inhibition of PI3K/AKT signalling was previously shown to induce morphological changes in other cell types, which is in line with the changes in adipose tissue cell size we observed [43]. In contrast to altering adipocyte morphology, wortmannin incubation did not significantly impact Pi3k-related gene expression (*Pcna*) or Akt phosphorylation.

Glut1, encoding a ubiquitous glucose transporter, has been shown to be induced upon insulin-mediated activation of Pi3K/Akt/mTor signalling in various cell lines [44]. Unexpectedly, in contrast to our previous results [9], we observed an approximately 5-fold upregulation of *Glut1* in lipomas after alpelisib incubation. Our results indicate that Pi3K/Akt/mTor pathway inhibition, with alpelisib, decreases both Akt phosphorylation and total Akt protein in lipoma tissue. *Glut1* increase could be a compensatory mechanism in response to alpelisib-induced PI3K/Akt/mTOR pathway inhibition, attempting to maintain glucose uptake and energy homoeostasis in lipoma cells.

Regarding genes related to lipolysis, we found that *Lipe* encoding hormone sensitive lipase (Hsl) was expressed at lower levels in lipomas than in control tissues. In contrast, *Pnpla2* encoding another major adipose tissue lipase, adipose triglyceride lipase (Atgl), remained unaltered [45,46]. Hsl is a key enzyme involved in the hydrolysis of triacylglycerols stored in adipocyte lipid droplets [47] and is a phosphorylation target of protein kinase A (Pka). PKA is inactivated through the reduction of intracellular cAMP levels by Akt-mediated activation of phosphodiesterase 3B (Pde3b) [48]. Therefore, inhibition of the Pi3K/Akt signalling pathway should increase Hsl phosphorylation and enhance lipolysis. Alpelisib application further decreased *Lipe* expression in lipoma tissues, which was confirmed at the protein level. This effect was specific, as the expression of *Pnpla2* encoding Atgl [45,46] remained unchanged. Other genes implicated in lipolysis regulation did not show consistent responses, with variable results for the expression of genes encoding lipolysis inhibitors (*Ptger3*, *Gnai*, *MaoA*, *MaoB*) [33,49].

As expected, alpelisib induced Hsl phosphorylation in both control and lipoma tissues, with a significantly higher phosphoHsl/Hsl ratio in lipomas. In line with the mRNA expression results, total Hsl protein was decreased in lipoma compared to that in control WAT. We generally observed a strong downregulation of all proteins tested after incubation with alpelisib, limiting the conclusions we are able to draw from these experiments.

Regarding murine tissue slice cultures, the functional outcome of the increased Hsl phosphorylation could not be determined by measuring glycerol release, as inhibitor treatment did not alter glycerol content in the supernatants of either tissue. To test whether HSL phosphorylation correlates with glycerol release in a different model, we used adipocytes isolated from human lipoma tissues obtained after surgical removal of sporadic lipomas from otherwise healthy subjects. Interestingly, in human adipocytes, we observed increased glycerol release following alpelisib treatment in one third of the samples (3 out of 9). Consequently, it would be valuable to investigate the factors that cause increased glycerol release in alpelisib-treated lipomas.

In summary, we established a tissue culture model allowing the incubation of lipoma and control tissue with Pi3k inhibitors for up to 3 days without compromising cell morphology or viability. Alpelisib significantly affected adipocyte size, gene expression and Pi3k/Akt/mTor pathway activation in lipomas compared to control WAT. Alpelisib treatment particularly affected proliferation and lipolysis markers, such as *Pparg, Lipe*, as well as phosphorylated and total Hsl proteins. Our results indicate that alpelisib may be a promising new treatment option for patients with PHTS-related lipomas. Despite

our promising findings, further *in vivo* validation is necessary to confirm alpelisib's therapeutic efficacy in the systemic context of PHTS-associated lipomas. Future research should explore long-term impacts of alpelisib in clinical trials and its combination with other PI3K inhibitors to optimize therapeutic outcomes.

Acknowledgments

We thank all donors for providing lipoma tissue samples. This work was supported by the Animal Core Facilities of the Leipzig University Faculty of Medicine and Saxon Incubator for Clinical Translation.

Disclosure statement

No potential conflict of interest was reported by the author(s).

Funding

This work was funded by the German Research Foundation (Deutsche Forschungsgemeinschaft, DFG) project number [209933838, CRC 1052/3], subprojects B4 (NK), B10 (DLD and AG), B12 (KK), and Z2 (open access publishing). We acknowledge the support from the Open Access Publishing Fund of Leipzig University, supported by the German Research Foundation within the programme Open Access Publication Funding.

Author contributions statement

L.M.M., K.W., S.K., A.H., S.R., S.G., N.K., K.K., W.K., D.LD., A.G. Conception: L.M.M., S.K., D.LD., A.G; study design: L. M.M., S.K., D.LD., A.G.; execution: S.G., N.K., K.K., W.K., S. R.; acquisition of data: L.M.M., S.R., A.H., N.K., K.K., A.G.; analysis and interpretation: L.M.M., K.W.,S.K., D.LD., A.G.; drafted or written: L.M.M., A.G.; substantially revised or critically reviewed the article: S.G., N.K., W.K., D.LD. All authors approved the submitted manuscript version.

Data availability statement

Raw data were generated at the University Hospital for Children and Adolescents, Center for Pediatric Research or the Institute of Anatomy, Leipzig University, Germany. All data that support the findings of this study are openly available in Zenodo at https://doi.org/10.5281/zenodo.13691359.

References

[1] Breiding MJ. PTEN hamartoma tumor syndromes. Physiol Behav. 2014;63(8):1–18. doi: 10.1038/ejhg.2008.162.PTEN

[2] Manning BD, Cantley LC. AKT/PKB signaling: navigating downstream. Cell. 2007;129(7):1261–1274. doi: 10.1016/j.cell.2007.06.009

[3] Hoxhaj G, Manning BD. The PI3K–AKT network at the interface of oncogenic signalling and cancer metabolism. Nat Rev Cancer. 2020;20(2):74–88. doi: 10.1038/s41568-019-0216-7

[4] Cantley LC, Neel BG. New insights into tumor suppression: PTEN suppresses tumor formation by restraining the phosphoinositide 3-kinase/akt pathway. Proc Natl Acad Sci USA. 1999;96(8):4240–4245. doi: 10.1073/pnas.96.8.4240

[5] LoPiccolo J, Ballas MS, Dennis PA. PTEN hamartomatous tumor syndromes (PHTS): rare syndromes with great relevance to common cancers and targeted drug development. Crit Rev Oncol Hematol. 2007;63(3):203–214. doi: 10.1016/j.critrevonc.2007.06.002

[6] Beretta M, Bauer M, Hirsch E. PI3K signaling in the pathogenesis of obesity: the cause and the cure. Adv Biol Regul. 2015;58:1–15. Elsevier Ltd. doi: 10.1016/j.jbior.2014.11.004

[7] Gorlin RJ, Cohen MM, Condon LM, et al. Bannayan-Riley-Ruvalcaba syndrome. Am J Med Genet. 1992;44(3):307–314. doi: 10.1002/ajmg.1320440309

[8] Drissen MMCM, Schieving JH, Schuurs-Hoeijmakers JHM, et al. Red flags for early recognition of adult patients with PTEN hamartoma tumour syndrome. Eur J Med Genet. 2021;64(12):104364. doi: 10.1016/j.ejmg.2021.104364

[9] Kirstein AS, Augustin A, Penke M, et al. The novel phosphatidylinositol-3-kinase (PI3K) inhibitor alpelisib effectively inhibits growth of PTEN-haploinsufficient lipoma cells. Cancers (Basel). 2019;11(10):1586. doi: 10.3390/cancers11101586

[10] Schmid GL, Kässner F, Uhlig HH, et al. Sirolimus treatment of severe PTEN hamartoma tumor syndrome: case report and in vitro studies. Pediatr Res. 2014;75(4):527–534. doi: 10.1038/pr.2013.246

[11] Ngeow J, Eng C. PTEN in hereditary and sporadic cancer. Cold Spring Harb Perspect Med. 2020;10(4):1–19. doi: 10.1101/cshperspect.a036087

[12] Furet P, Guagnano V, Fairhurst RA, et al. Discovery of NVP-BYL719 a potent and selective phosphatidylinositol-3 kinase alpha inhibitor selected for clinical evaluation. Bioorg Med Chem Lett. 2013;23(13):3741–3748. doi: 10.1016/j.bmcl.2013.05.007

[13] André F, Ciruelos E, Rubovszky G, et al. Alpelisib for PIK3CA -Mutated, hormone receptor–positive advanced breast cancer. N Engl J Med. 2019;380(20):1929–1940. doi: 10.1056/nejmoa1813904

[14] Venot Q, Blanc T, Rabia SH, et al. Targeted therapy in patients with PIK3CA-related overgrowth syndrome. Nature. 2018;558(7711):540–546. doi: 10.1038/s41586-018-0217-9

[15] Garreta Fontelles G, Pardo Pastor J, Grande Moreillo C. Alpelisib to treat CLOVES syndrome, a member of the PIK3CA-related overgrowth syndrome spectrum. Br J Clin Pharmacol. 2022;88(8):3891–3895. doi: 10.1111/bcp.15270

[16] Morin G, Degrugillier-Chopinet C, Vincent M, et al. Treatment of two infants with PIK3CA-related overgrowth spectrum by alpelisib. J Exp Med. 2022;219(3):1–8. doi: 10.1084/jem.20212148

[17] Pagliazzi A, Oranges T, Traficante G, et al. PIK3CA-Related overgrowth spectrum from diagnosis to

targeted therapy: a case of CLOVES syndrome treated with alpelisib. Front Pediatr. 2021;9(September):1–6. doi: 10.3389/fped.2021.732836

[18] Madsen RR, Semple RK. PIK3CA-related overgrowth: silver bullets from the cancer arsenal? Trends Mol Med. 2022;28(4):255–257. doi: 10.1016/j.molmed.2022.02.009

[19] López Gutiérrez JC, Lizarraga R, Delgado C, et al. Alpelisib treatment for genital vascular malformation in a patient with congenital lipomatous overgrowth, vascular malformations, epidermal nevi, and spinal/skeletal anomalies and/or scoliosis (CLOVES) syndrome. J Pediatr Adolesc Gynecol. 2019;32(6):648–650. doi: 10.1016/j.jpag.2019.07.003

[20] Bowles DW, Ma WW, Senzer N, et al. A multicenter phase 1 study of PX-866 in combination with docetaxel in patients with advanced solid tumours. Br J Cancer. 2013;109(5):1085–1092. doi: 10.1038/bjc.2013.474

[21] Levy B, Spira A, Becker D, et al. A randomized, phase 2 trial of docetaxel with or without PX-866, an irreversible oral phosphatidylinositol 3-kinase inhibitor, in patients with relapsed or metastatic non-small-cell lung cancer. J Thorac Oncol. 2014;9(7):1031–1035. doi: 10.1097/JTO.0000000000000183

[22] Filtz EA, Emery A, Lu H, et al. Rb1 and Pten co-deletion in osteoblast precursor cells causes rapid lipoma formation in mice. PLOS ONE. 2015;10(8):1–15. doi: 10.1371/journal.pone.0136729

[23] Walkley CR, Qudsi R, Sankaran VG, et al. Conditional mouse osteosarcoma, dependent on p53 loss and potentiated by loss of Rb, mimics the human disease. Genes Dev. 2008;22(12):1662–1676. doi: 10.1101/gad.1656808

[24] Sage J, Miller AL, Pérez-Mancera PA, et al. Acute mutation of retinoblastoma gene function is sufficient for cell cycle re-entry. Nature. 2003;424(6945):223–228. doi: 10.1038/nature01764

[25] Lesche R, Groszer M, Gao J, et al. Cre/loxP-mediated inactivation of the murine Pten tumor suppressor gene. Genesis. 2002;32(2):148–149. doi: 10.1002/gene.10036

[26] Rodda SJ, McMahon AP. Distinct roles for Hedgehog and canonical Wnt signaling in specification, differentiation and maintenance of osteoblast progenitors. Development. 2006;133(16):3231–3244. doi: 10.1242/dev.02480

[27] Trotman LC, Niki M, Dotan ZA, et al. Pten dose dictates cancer progression in the prostate. PLOS Biol. 2003;1(3):385–396. doi: 10.1371/journal.pbio.0000059

[28] Schopow N, Kallendrusch S, Gong S, et al. Examination of ex-vivo viability of human adipose tissue slice culture. PLOS ONE. 2020;15(5):1–17. doi: 10.1371/journal.pone.0233152

[29] Haehnel S, Reiche K, Loeffler D, et al. Deep sequencing and automated histochemistry of human tissue slice cultures improve their usability as preclinical model for cancer research. Sci Rep. 2019;9(1):1–15. doi: 10.1038/s41598-019-56509-5

[30] Kässner F, Kirstein A, Händel N, et al. A new human adipocyte model with PTEN haploinsufficiency. Adipocyte. 2020;9(1):290–301. doi: 10.1080/21623945.2020.1785083

[31] Landgraf K, Rockstroh D, Wagner IV, et al. Evidence of early alterations in adipose tissue biology and function and its association with obesity-related inflammation and insulin resistance in children. Diabetes. 2015;64(4):1249–1261. doi: 10.2337/db14-0744

[32] Schindelin J, Arganda-Carreras I, Frise E, et al. Fiji: an open-source platform for biological-image analysis. Nat Methods. 2012;9(7):676–682. doi: 10.1038/nmeth.2019

[33] Le Duc D, Lin CC, Popkova Y, et al. Reduced lipolysis in lipoma phenocopies lipid accumulation in obesity. Int J Obes. 2021;45(3):565–576. doi: 10.1038/s41366-020-00716-y

[34] Chakrabarti P, English T, Shi J, et al. Mammalian target of rapamycin complex 1 suppresses lipolysis, stimulates lipogenesis, and promotes fat storage. Diabetes. 2010;59(4):775–781. doi: 10.2337/db09-1602

[35] Kirstein AS, Kehr S, Nebe M, et al. PTEN regulates adipose progenitor cell growth, differentiation, and replicative aging. J Biol Chem. 2021;297(2):100968. doi: 10.1016/j.jbc.2021.100968

[36] Ladraa S, Zerbib L, Bayard C, et al. PIK3CA gain-of-function mutation in adipose tissue induces metabolic reprogramming with Warburg-like effect and severe endocrine disruption. Sci Adv. 2022;8(49):1–18. doi: 10.1126/sciadv.ade7823

[37] Suga H, Eto H, Inoue K, et al. Cellular and molecular features of lipoma tissue: comparison with normal adipose tissue. Br J Dermatol. 2009;161(4):819–825. doi: 10.1111/j.1365-2133.2009.09272.x

[38] Kim JE, Shepherd PR, Chaussade C. Investigating the role of class-ia PI 3-kinase isoforms in adipocyte differentiation. Biochem Biophys Res Commun. 2009;379(4):830–834. doi: 10.1016/j.bbrc.2008.12.089

[39] Foukas LC, Claret M, Pearce W, et al. Critical role for the p110α phosphoinositide-3-oh kinase in growth and metabolic regulation. Nature. 2006;441(7091):366–370. doi: 10.1038/nature04694

[40] Zhang B, Luk C, Valadares J, et al. Dominant role of pi3k p110α over p110β in insulin and β-adrenergic receptor signalling. Int J Mol Sci. 2021;22(23):12813. doi: 10.3390/ijms222312813

[41] Hashimoto M, Rao S, Tokuno O, et al. DNA-PK: the major target for wortmannin-mediated radiosensitization by the inhibition of DSB repair via NHEJ pathway. J Radiat Res. 2003;44(2):151–159. doi: 10.1269/jrr.44.151

[42] Liu Y, Jiang N, Wu J, et al. Polo-like kinases inhibited by Wortmannin: labeling site and downstream effects. J Biol Chem. 2007;282(4):2505–2511. doi: 10.1074/jbc.M609603200

[43] Tsuji-Tamura K, Ogawa M. Inhibition of the PI3K-Akt and mTORC1 signaling pathways promotes the elongation of vascular endothelial cells. J Cell Sci. 2016;129(6):1165–1178. doi: 10.1242/jcs.178434

[44] Taha C, Liu Z, Jin J, et al. Opposite translational control of GLUT1 and GLUT4 glucose transporter mRNAs in response insulin. Role of mammalian target of rapamycin, protein kinase B, and phosphatidylinositol 3-kinase in GLUT1 mRNA translation. J Biol Chem. 1999;274(46):33085–33091. doi: 10.1074/jbc.274.46.33085

[45] Althaher AR, Cheng JT. An overview of hormone-sensitive lipase (HSL). Sci World J. 2022;2022:1–9. doi: 10.1155/2022/1964684
[46] Ahmadian M, Wang Y, Sul HS. Medicine in focus: lipolysis in adipocytes. Int J Biochem Cell Biol. 2010;42(5):555–559. doi: 10.1016/j.biocel.2009.12.009
[47] Zechner R, Zimmermann R, Eichmann TO, et al. FAT SIGNALS - Lipases and lipolysis in lipid metabolism and signaling. Cell Metab. 2012;15(3):279–291. doi: 10.1016/j.cmet.2011.12.018
[48] Duncan RE, Ahmadian M, Jaworski K, et al. Regulation of lipolysis in adipocytes. Annu Rev Nutr. 2007;27(1):79–101. doi: 10.1146/annurev.nutr.27.061406.093734
[49] Roh E, Yoo HJ. The role of adipose tissue lipolysis in diet-induced obesity: focus on vimentin. Diabetes Metab J. 2021;45(1):43–45. doi: 10.4093/DMJ.2020.0293